

1           **Estimation of submarine groundwater discharge in Plover**  
2                           **Cove, Tolo Harbour, Hong Kong by <sup>222</sup>Rn**

3  
4                           Kiu Chung Tse, Jiu Jimmy Jiao\*

5                           Department of Earth Sciences, the University of Hong Kong,  
6                           Hong Kong Special Administrative Region, China

7  
8           \*Corresponding author  
9  
10

11   **Abstract**

12           Algal blooms in Tolo Harbour, Hong Kong have received much attention and  
13           submarine groundwater discharge is speculated to be a significant pathway carrying  
14           nutrients into the constricted estuary. Plover Cove, a small cove in the Harbour, was  
15           selected for SGD analysis using <sup>222</sup>Rn budget. The volumetric SGD rates are estimated to  
16           be **about 8,000 m<sup>3</sup>/day** for neap tide and **about 17,000 m<sup>3</sup>/day** for spring tide. Result of  
17           nutrient analysis of the porewater indicates that the nutrient loading through this pathway  
18           is speculated to be crucial for eutrophication in Tolo Harbour. Current practice for the  
19           management of algal blooms in Hong Kong, in which nutrient loading through SGD was  
20           ignored, has to be reviewed and the control measures of groundwater contamination are  
21           obviously required.

22  
23   Index terms: Geochemical tracers; Groundwater hydrology; Groundwater transport;  
24   Hydrological cycles and budgets; Pollution: urban, regional and global.

25

## 26 **Introduction**

27 Tolo Harbour is located in the northeastern part of Hong Kong's New Territories  
28 (Figure 1). It is susceptible to pollution because of the bottlenecked coastline  
29 configuration as well as the prevailing northeasterly wind direction (Yin, 2003). Current  
30 is low for the harbour and the estimated water residence times in the inner harbour range  
31 from 16-42 days (Hodgkiss and Yim, 1995). All these factors result in preventing the  
32 pollutants to be removed effectively. While the harbour is already under stress due to  
33 natural factors, urban development since 1970s has further deteriorated the water quality.  
34 Dramatic expansion of human population, from 70 000 in 1973 to 1 000 000 in 1990, has  
35 degraded the environment.

36 As a consequence, algal bloom incidents increased from 1 per year in 1978 to over 40  
37 in 1988 (Holmes, 1988; Environmental Protection Department (EPD), 2004). Holmes  
38 (1988) has attributed the environmental degradation to reduction of the mangrove  
39 coastline through the process of land reclamation. The mangrove coastline serves as an  
40 effective sink for nutrients, so the loss of this natural resource shifts the primary  
41 biological productivity to planktonic algae.

42 In order to alleviate the pollutant loading on Tolo Harbour, the government has  
43 enforced the Tolo Harbour Action Plan in 1988 which included livestock waste control,  
44 sewage treatment modification, effluent export scheme, legislation enforcement and  
45 landfill restoration. An ecosystem model, which was developed for the Hong Kong  
46 government, claimed that the concentrations of ammonia and nitrate could drop to zero  
47 after the Action Plan was implemented (Holmes, 1988). After the action plan has been  
48 implemented, the number of algal bloom incidents has been decreased to ~10 incidents  
49 per year. The total phytoplankton densities, however, were still 2-6 times higher at

50 stations in Tolo Harbour and Channel than those in other water control zones over Hong  
51 Kong (EPD, 2004). Xu et al. (2004) showed that the loadings of total phosphorus and  
52 total nitrogen in Tolo Harbour even reached another peaks in 1996 and 1998 respectively.  
53 It is speculated that the phytoplankton may be sustained by nutrients from other sources.

54 Hodgkiss and Ho (1997) suggested that implementation of the Tolo Harbour Action  
55 Plan resulted in a lower N:P ratio which led to a shift in algal species composition from  
56 diatoms to dinoflagellates and the dominance of dinoflagellates was the major cause of  
57 the dramatic increase in red tide occurrence. This replacement of algal species was neither  
58 found by Yung et al. (1997) nor supported by the long-term monitoring by EPD. Hu et al.  
59 (2001) conducted a sediment diffusion experiment by placing undisturbed sediment core  
60 into a settling column in laboratory and adding water sample collected from  
61 corresponding site. They demonstrated that sediments can release 0.5 mmol of  
62 orthophosphate phosphorus and 2.2 mmol of nitrate-nitrite nitrogen per square metre per  
63 day.

64 Recently research in other coastal areas indicates that the direct discharge of  
65 groundwater into the coastal zone may be a potentially significant pathway of dissolved  
66 nutrients into the coastal environment (Laroche et al., 1997; Griggs et al., 2003; Miller  
67 and Ullman, 2004). Terrestrial groundwater can discharge into the sea directly in response  
68 to the hydraulic gradient, with groundwater head higher than sea level (Johannes, 1980).  
69 Li and Jiao (2002) proposed a tide-induced seawater-groundwater circulation that SGD  
70 happens even in the absence of net inland recharge of groundwater.

71 It is speculated that eutrophication in Tolo Harbour may be attributed to the nutrient  
72 fluxes through the pathway of submarine groundwater discharge (SGD). Tolo Harbour is  
73 enclosed by such a large catchment that the amount of SGD is believed to be comparable  
74 to the river water flux. This study focused on Plover Cove that has no major river system.

75 Plover Cove is adjacent to a mountain range including Wong Leng (639 m) and Pat Sin  
76 Leng (500-600 m), with a surface area of around 4 km<sup>2</sup> (Figure 1). Radium study was  
77 conducted for Tolo Harbour (Tse, 2006) and based on this radium study, Plover Cove is  
78 identified as a key area in Tolo Harbour receiving potentially significant amount of SGD  
79 and details of the radium study can be found in Tse (2006). The current paper focuses on  
80 radon study and the SGD flux was estimated by <sup>222</sup>Rn following the approach described  
81 by Burnett and Dulaiova (2003).

## 82 **Background of the Site**

83 The overall surface area for Tolo Harbour is 52 km<sup>2</sup> including the part of Tolo  
84 Channel. In the inner harbour the water depth is less than 10m, while along the channel  
85 the average depth is about 12 m. The mean sea level is 1.15 m above Principal Datum  
86 (mPD), with average diurnal tidal range of 0.97 m (EPD, 1994). There are several rivers  
87 entering Tolo Harbour and according to the monitoring data between 1998 and 2004 from  
88 EPD, the total annual discharge rate is 3.61 x 10<sup>10</sup> m<sup>3</sup>/yr. The mean annual rainfall is  
89 2214 mm.

90 Tolo Harbour is enclosed by a large catchment with an area of 50 km<sup>2</sup>. The catchment  
91 is formed by three main mountainous blocks divided by the new towns Tai Po and Sha  
92 Tin. The geology was described in detail by Tam (1980), Addison (1986) and Lai et al.  
93 (1996). The district is formed mainly of Mesozoic stratified pyroclastic rocks sandwiched  
94 between the Mesozoic sedimentary rocks, with sandstone, siltstone and conglomerate  
95 above and marine mudstone and siltstone below.

96 The volcanic rocks are intruded by a complex granitic pluton at the age of Late  
97 Jurassic to Early Cretaceous, which crops out at the low-lying areas. A series of faults  
98 trending northeast and northwest was generated and one of the biggest faults is the Lai

99 Chi Kok – Tolo Channel Fault which belongs to a fault zone extending across Sha Tin  
100 Valley to Tolo Channel.

101 The superficial soils, including the mantle of weathered rock, colluvium, alluvium and  
102 beach sand are considered as shallow unconfined aquifer, which can be over 20 m thick  
103 (Ruxton and Berry, 1957). The sandy deposit is subsequently replaced by silt or marine  
104 mud in the estuary which serves as an extensive layer of aquitard. There are successive  
105 layers of marine and alluvial deposits underlain the Holocene marine mud, which  
106 indicates that channelized sand bodies can be found offshore as confined aquifers. These  
107 channels are potentially fresh if they are hydraulically connected with the recharge area  
108 onshore.

109 The bedrock, according to the degree of decomposition, varies from fresh rock to  
110 residual soil. Fracture zones exist along the rockhead below the decomposed rock which  
111 form a relatively deep confined aquifer (Jiao et al., 2005; Jiao et al., 2006).

112 Grant (1989) investigated the permeability in Lam Tsuen and Tolo Harbour Areas and  
113 in his study, the permeabilities of alluvial plain and terrace lands are  $1.17 \times 10^{-4}$  m/s and  
114  $2.17 \times 10^{-4}$  m/s respectively.

115

## 116 **Methodology**

117 The SGD flux was estimated by  $^{222}\text{Rn}$  following the approach described by Burnett  
118 and Dulaiova (2003). In general,  $^{222}\text{Rn}$  concentration in the system is influenced by  
119 various sources and sinks, such as ingrowth from  $^{226}\text{Ra}$  dissolved in the water, tidal effect,  
120 atmospheric loss, diffusion from sediments, mixing loss to the open sea and SGD (Figure  
121 2). An increase or decrease of  $^{222}\text{Rn}$  concentration over a time interval is referred to the  
122 net balance between these sources and sinks during that period.  $^{222}\text{Rn}$  concentrations in  
123 coastal waters are measured continuously to determine the difference between two

124 successive measurements. This is then corrected for all other sources and sinks to obtain  
125 the  $^{222}\text{Rn}$  flux attributed to SGD. With this flux divided by  $^{222}\text{Rn}$  concentration in fresh  
126 groundwater or porewater, the SGD flux is computed.

$$127 \quad F_{SGD} = F_t - F_{sed} - F_o + F_{atm} + F_i + F_m \quad (1)$$

128 where  $F_{SGD}$  is the  $^{222}\text{Rn}$  flux attributed to SGD

129  $F_t$  is the difference in concentrations of excess  $^{222}\text{Rn}$  between two successive  
130 hours

131  $F_{sed}$  is the flux diffused from sediments

132  $F_o$  is the flux leaving with the outgoing tide

133  $F_{atm}$  is the flux into the atmosphere

134  $F_i$  is the flux entering with the incoming tide

135  $F_m$  is the flux out of the system by mixing

136 A site in Plover Cove was selected for  $^{222}\text{Rn}$  analysis in July 2005.  $^{222}\text{Rn}$  in coastal  
137 waters was monitored continuously by a commercially available radon-in-air monitoring  
138 system called RAD7 produced by DurrIDGE Co., Inc. for four days, with 48 hours during  
139 the neap tide (14-16 July) and 48 hours during the spring tide (21-23 July). In the  
140 meantime, water depth was estimated from the iron framework where a height indicator  
141 was made. Water samples were collected bihourly for  $^{226}\text{Ra}$  analysis. Sediments were  
142 collected from the sea bottom to estimate  $^{222}\text{Rn}$  in porewater. Wind speed, salinity, air and  
143 water temperatures were measured manually every 10 minutes. At the same time, a  
144 continuous heat-type automated seepage meter (Taniguchi and Iwakawa, 2001) was also  
145 deployed for direct SGD measurement. It was pushed into the sea bottom and  
146 programmed to take readings every 6 s. During the sampling period, monitoring of  $^{222}\text{Rn}$   
147 in coastal waters was suspended twice: from 00:23, July 16 onwards to measure  $^{222}\text{Rn}$  in  
148 ambient air, and from 05:00, July 22 onwards because of a storm.  $^{222}\text{Rn}$  in groundwater

149 from two private wells (Po Sum Pai and Chim Uk) was collected and measured in March  
150 2006. Po Sum Pai private well is situated on Quaternary deposits of volcanic rocks with a  
151 depth of 2.7 m, while Chim Uk private well is situated on granitic rocks with a depth of  
152 3.3 m.

### 153 **Continuous Monitoring of $^{222}\text{Rn}$**

154 In order to monitor  $^{222}\text{Rn}$  in coastal waters continuously, an iron framework was  
155 placed on the sea bottom on which the submersible pump was fastened so that it was  
156 fixed at 0.5 m above the sea bottom. Seawater was pumped out and filtered through a 1  
157  $\mu\text{m}$  cartridge filter to screen out the particulates. It was then sparged into an air-water  
158 exchanger where radon was distributed from the running flow of water to a closed air  
159 loop until the two phases reached equilibrium. The air stream was then fed to the RAD7  
160 for measurement, which was converted to  $^{222}\text{Rn}$  in the water by the following equation  
161 (Durridge Co., Inc., 2001),

$$162 \qquad \qquad \qquad \alpha = 0.105 + 0.405e^{-0.050T} \qquad \qquad \qquad (2)$$

163

164 where  $\alpha$  is the partition coefficient (concentration ratio of water to air)

166  $T$  is the water temperature in  $^{\circ}\text{C}$ , which was measured by a temperature probe  
167 inserted into the air-water exchanger

168 The RAD7 was programmed to integrate counts every hour.

### 169 **$^{226}\text{Ra}$ analysis**

170 The water from the air-water exchanger was fed into a 50 L water tank for radium  
171 extraction. After 50 L of the water had been collected, it was forced to flow through 30 g  
172 of Mn-fiber described by Moore (1976) to extract the radionuclide. The flow rate was  
173 controlled below 1 L/min so that sufficient time was allowed for the adsorption. In the  
174 laboratory,  $^{226}\text{Ra}$  was extracted from the Mn-fiber by refluxing with HCl, and the filtrate

175 was co-precipitated with 10 mL of saturated  $\text{Ba}(\text{NO}_3)_2$  and 25 mL of 7 M  $\text{H}_2\text{SO}_4$ . The  
176 precipitate [ $\text{Ba}(\text{Ra})\text{SO}_4$ ] was then filtered out by 0.45  $\mu\text{m}$  glass-fiber filter and washed  
177 with 3 M HCl and water to remove the Mn remains. Finally the precipitant was air-dried,  
178 stored in a small vial for 3-4 weeks for equilibrium, and measured by gamma ray  
179 spectrometer (Rutgers van der Loeff and Moore,1999).

## 180 **Determination of $^{222}\text{Rn}$ in Groundwater**

181 Groundwater samples were pumped out from two private wells (Figure 1) and  
182 collected in 250 mL collection vials. As radon in groundwater can be quickly distributed  
183 into air, narrow tubing was attached to the pump and inserted into the bottom of the  
184 collection vial which was placed inside a 1 L plastic beaker. The vial was filled from  
185 bottom with fresh sample until the water overflowed into the beaker and the water in the  
186 beaker rose well above the vial. In this way, the vial was flushed with fresh sample  
187 without exposure to air and it was capped while still under the water.

188 The samples were then measured by RAD7 with the RAD- $\text{H}_2\text{O}$  accessory. RAD- $\text{H}_2\text{O}$   
189 aerates the sample for 5 minutes to deliver  $^{222}\text{Rn}$  to the RAD7. The system will wait a  
190 further 5 minutes for the equilibrium between  $^{222}\text{Rn}$  and  $^{218}\text{Po}$ . The air stream is then  
191 measured by RAD7 in 4 runs of five-minute period and the result is given as the average  
192 of the 4 runs.

## 193 **Determination of $^{222}\text{Rn}$ in Porewater**

194 Concentration of  $^{222}\text{Rn}$  in porewater was determined by sediment equilibration  
195 experiment which was described by Corbett et al. (1998). Sediments from the sea bottom  
196 and seawater were collected for the experiment. In the laboratory, 85 g sediments were  
197 mixed with 300 mL seawater in a 500-mL Erlenmeyer flask. The flask was sealed and  
198 agitated for 1 month until  $^{222}\text{Rn}$  in head space, water and sediments reach equilibrium.  
199 The water was then pumped out and transferred into a 40 mL collection vial, with the

200 special sampling technique employed to prevent air contact. The sample was then  
201 measured by RAD7 with the RAD-H<sub>2</sub>O accessory.

## 202 **Determination of Nutrients in Porewater**

203 Wet sediment at a depth of 0.5 m was collected along the foreshore during lowest tide.  
204 It was immediately brought to the laboratory where the porewater was separated from the  
205 sediment by centrifuge. Nutrients in porewater (NO<sub>2</sub>-N, NO<sub>3</sub>-N, NH<sub>3</sub>-N, PO<sub>4</sub>-P and silica)  
206 were then analyzed by a spectrophotometer.

207

## 208 **Result and Discussion**

209 The results of the continuous <sup>222</sup>Rn measurements in the water column, together with  
210 the observed water depth, during the neap and spring tides are shown in Figures 3 and 4,  
211 respectively. The concentrations of <sup>222</sup>Rn were high during low tide, and low during high  
212 tide, which fluctuated between 110 and 688 Bq/m<sup>3</sup> with an average of 222 Bq/m<sup>3</sup>. Tidal  
213 period cyclicity of the <sup>222</sup>Rn data was generally accepted to reflect dilution of offshore  
214 waters at flood tide, mixing offshore and most importantly, SGD variation (Kim and  
215 Hwang, 2002; Burnett and Dulaiova, 2003; Lambert and Burnett, 2003). At low tide,  
216 recirculated seawater drains out due to tidal pumping. Simultaneously the hydrostatic  
217 pressure is lowered and the hydraulic gradient between seawater and groundwater is  
218 increased, which contributes to a larger SGD flux. At high tide, recirculated seawater  
219 seeps into the seabed sediments due to tidal pumping. Simultaneously the hydrostatic  
220 pressure is increased and the hydraulic gradient between seawater and groundwater is  
221 decreased, which contributes to a smaller SGD flux.

## 222 **Tidal Effects**

223 In order to account for the dilution effect during flood tide, Lambert and Burnett  
224 (2003) introduced the concept of excess <sup>222</sup>Rn inventory to eliminate the effect. Excess

225  $^{222}\text{Rn}$  inventory is defined as the product of excess  $^{222}\text{Rn}$  in water (Concentration of  
226  $^{222}\text{Rn}$  – Concentration of  $^{226}\text{Ra}$ ) and the water depth ( $h$ ). During flood tide, a larger  $h$  is  
227 multiplied so that the dilution effect can be compensated. Apart from that,  $^{226}\text{Ra}$  which is  
228 about  $6 \text{ Bq/m}^3$  was also subtracted from  $^{222}\text{Rn}$  in excess  $^{222}\text{Rn}$  inventory so that the radon  
229 supported by  $^{226}\text{Ra}$  was also corrected.

230 Excess  $^{222}\text{Rn}$  inventory can actually be interpreted as the excess  $^{222}\text{Rn}$  in a water  
231 column within an area of  $1 \text{ m}^2$ . From this definition, it is deduced that inventory is still  
232 subject to changes in tidal height:  $^{222}\text{Rn}$  is removed from the water column with the  
233 outgoing waters on the ebb tide ( $F_o$ ) while extra  $^{222}\text{Rn}$  is added to the water column with  
234 the incoming waters on the flood tide ( $F_i$ ). Correction is required to remove this tidal  
235 effect. The excess  $^{222}\text{Rn}$  inventory is corrected by an addition of the removed  $^{222}\text{Rn}$   
236 inventory ( $\Delta h \times$  concentration of  $^{222}\text{Rn}$  in the study domain) at low tide or a subtraction of  
237 the extra  $^{222}\text{Rn}$  inventory ( $\Delta h \times$  concentration of  $^{222}\text{Rn}$  in offshore waters) at high tide,  
238 where  $\Delta h$  is the difference between the two successive tidal heights.

### 239 **Atmospheric Loss**

240  $^{222}\text{Rn}$  is slightly soluble gas in water, exchange across the air-water interface is  
241 possible if  $^{222}\text{Rn}$  in the two phases are in disequilibrium. At equilibrium,

$$242 \quad \quad \quad 243 \quad \quad \quad C_w = \alpha C_a \quad (3)$$

244 where  $C_w$  is the concentration of  $^{222}\text{Rn}$  in water

246  $C_a$  is the concentration of  $^{222}\text{Rn}$  in air

247  $\alpha$  is the partition coefficient

248 When  $C_w > \alpha C_a$ ,  $^{222}\text{Rn}$  will diffuse across the air-water interface and according to  
249 MacIntyre et al. (1995), the diffusive flux is,

250

251 
$$F_{atm} = k(C_w - \alpha C_a) \quad (4)$$

252 where  $F_{atm}$  is the diffusive flux across the air-water interface

254  $k$  is the gas transfer velocity

255 Considerable effort has gone into determining empirical relationship between the gas  
 256 transfer velocity and wind speed, which was based on five experiments on lakes with  
 257 deliberate tracers SF<sub>6</sub> (MacIntyre et al., 1995; Lambert and Burnett, 2003),

258

259 
$$k_{600} = \begin{cases} 0.45\mu^{1.6} \left(\frac{Sc}{600}\right)^{-0.5} & \text{for } \mu > 3.6 \text{ m/s} \\ 0.45\mu^{1.6} \left(\frac{Sc}{600}\right)^{-0.6667} & \text{for } \mu \leq 3.6 \text{ m/s} \end{cases} \quad (5)$$

260 where  $\mu$  is the measured wind speed (m/s)

262  $Sc$  is the Schimidt number

263  $k_{600}$  is the gas transfer velocity normalized to the Schimidt number of CO<sub>2</sub> at 20  
 264 °C in freshwater (cm/hr)

265 At wind speeds of less than 1.5 m/s, the value for  $k$  is assumed to be 0.91 cm/hr  
 266 (Lambert and Burnett, 2003). This value is calculated based on the  $k$  value for CH<sub>4</sub> (0.75  
 267 ± 0.54 cm/hr) measured by Happell et al. (1995) at zero wind speed.

268 The Schmidt number for <sup>222</sup>Rn in seawater is given by Pilson (1998) as a function of  
 269 the water temperature.

270 Five measurements were made from 23:40, July 15 to the end of neap tide period for  
 271 <sup>222</sup>Rn in air and the average (30 Bq/m<sup>3</sup>) is used for calculation (Table 1). Figures 5 and 6  
 272 show the temporal variations of wind speed and the diffusive flux of <sup>222</sup>Rn across the air-  
 273 water interface during the two sampling periods.

## 274 **Diffusive Flux from Seabed Sediments**

275 Similar to the air-water interface, exchange across the sediment-water interface is  
276 possible if concentration of  $^{222}\text{Rn}$  in porewater is greater than that in the overlying water.

277 The diffusive flux across the sediment-water interface is given by Martens et al. (1980),

$$278 \quad \quad \quad 279 \quad \quad \quad F_{sed} = (\lambda D_s)^{0.5} (C_{eq} - C_o) \quad (6)$$

280 where  $F_{sed}$  is the diffusive flux across the sediment-water interface

282  $\lambda$  is the decay constant of  $^{222}\text{Rn}$ , which is  $0.181 \text{ day}^{-1}$

283  $D_s$  is the effective wet bulk sediment diffusion coefficient

284  $C_{eq}$  is the concentration of  $^{222}\text{Rn}$  in porewater

285  $C_o$  is the concentration of  $^{222}\text{Rn}$  in the overlying water

286 Ullman and Aller (1981) pointed out that the effective wet bulk sediment diffusion  
287 coefficient is approximately equal to the product of porosity and the molecular diffusivity  
288 coefficient of  $^{222}\text{Rn}$ . Molecular diffusivity coefficient was described by Peng et al. (1974)  
289 as a function of temperature,

$$290 \quad \quad \quad 291 \quad \quad \quad D_o = 10^{-\left[\left(\frac{980}{T+273}\right)^{+1.59}\right]} \quad (7)$$

292 where  $D_o$  is the molecular diffusivity coefficient

294  $T$  is the temperature in  $^{\circ}\text{C}$

295 Particle size analysis classified the seabed sediments as loose uniform sand. The  
296 porosity estimated from soil analysis is around 0.41.

297 Concentration of  $^{222}\text{Rn}$  in porewater was determined by sediment equilibration  
298 experiment. From the experiment, the activity of  $^{222}\text{Rn}$  released from the wet sediments is  
299 0.6 Bq/kg. Concentration of  $^{222}\text{Rn}$  in porewater is calculated by,

300

301

$$C_{eq} = \frac{{}^{222}\text{Rn released from the wet sediment} \times \rho_{wet}}{n} \quad (8)$$

302 where  $n$  is the porosity (0.41)

303  $\rho_{wet}$  is the wet bulk density, which is measured as 2086 kg/m<sup>3</sup>, which is based on

304 excavation method and sand displacement test.

305 From the sediment equilibration experiment, concentration of <sup>222</sup>Rn in porewater is

306 estimated to be 3052 Bq/m<sup>3</sup>. Concentration of <sup>222</sup>Rn in overlying water was monitored

307 continuously during the two sampling periods. The diffusive flux of <sup>222</sup>Rn across the

308 sediment-water interface is calculated to be 0.4 Bq/m<sup>2</sup>·hr, which is insignificant in

309 comparison to the total flux.

### 310 **Mixing Loss**

311 Figures 7 and 8 show the net <sup>222</sup>Rn flux after correcting for atmospheric loss and

312 sediment diffusion, which should be a balance between supply from SGD and mixing loss

313 to the open sea. Burnett and Dulaiova (2003) and Lambert and Burnett (2003) chose the

314 negative net <sup>222</sup>Rn fluxes as conservative estimates of the mixing loss. Indeed a larger

315 mixing loss is possible to be balanced by a larger supply from SGD, but the conservative

316 estimates of the mixing loss provide a good guess for the minimum SGD flux. It is

317 represented by the dashes line shown in Figures 7 and 8.

318 The estimated mixing losses are between 29.4 to 89.0 Bq/m<sup>2</sup>·h r during neap tide and

319 between 64.0 to 125.0 Bq/m<sup>2</sup>·h r during spring tide.

### 320 **SGD Flux**

321 As mentioned, the net <sup>222</sup>Rn flux is a balance between supply from SGD and mixing

322 loss to the open sea. After correcting for mixing loss, the <sup>222</sup>Rn flux is solely attributed to

323 SGD. The average <sup>222</sup>Rn flux solely attributed to SGD is 52.8 Bq/m<sup>2</sup>·h r, which is about

324 130 times larger than the flux diffused from sediment. Although Hu et al. (2001) and Xu

325 et al. (2004) suggested that significant amount of nutrients was diffused from seabed  
326 sediments and supplied to the phytoplankton in Tolo Harbour, nutrients discharged with  
327 SGD are conceived to be much more significant than diffusion from sediment in Plover  
328 Cove.

329 In order to convert  $^{222}\text{Rn}$  fluxes to SGD fluxes, the  $^{222}\text{Rn}$  fluxes solely attributed to  
330 SGD have to be divided by the concentration of  $^{222}\text{Rn}$  in the SGD fluid. Determination of  
331 the SGD fluid requires an understanding of the discharge characteristic: If slow seepage  
332 through sediment is dominant,  $^{222}\text{Rn}$  in porewater will be a good guess of that in SGD;  
333 otherwise  $^{222}\text{Rn}$  in groundwater will be more representative if fast groundwater flow is  
334 dominant.  $^{222}\text{Rn}$  in porewater was determined by sediment equilibration experiment to be  
335  $3052 \text{ Bq/m}^3$ . Groundwater was collected from two private wells near Plover Cove, the  
336 concentrations of  $^{222}\text{Rn}$  are  $6858 \text{ Bq/m}^3$  ( $n = 28$ ;  $\sigma = 3728$ ) for Po Sum Pai private well  
337 and  $16790 \text{ Bq/m}^3$  ( $n = 5$ ;  $\sigma = 4188$ ) for Chim Uk private well.

338 The SGD fluxes are plotted on Figures 9 and 10 and summarized in Table 2. The  
339 inverse relationship between tidal height and SGD is verified. Precisely the peaks of SGD  
340 coincide with the transitions from flood tide to ebb tide. With porewater being selected to  
341 represent the SGD fluid, the mean SGD fluxes are 30.3 and 63.0 cm/day for neap and  
342 spring tides respectively. The mean SGD fluxes are 7.8 and 16.3 cm/day for neap and  
343 spring tides with groundwater from the two wells averaged to represent the SGD fluid.

344 The SGD fluxes based on terrestrial groundwater are chosen for calculating the  
345 nutrient loading to Plover Cove through SGD so as to obtain the most conservative  
346 estimates of SGD and the corresponding nutrient loading to Plover Cove. These values  
347 are also comparable to the mean SGD fluxes measured directly by seepage meter, which  
348 are 8.0 and 9.3 cm/day for neap and spring tides respectively.

349 The width of the seepage face is difficult to estimate. During the field studies, neap  
350 tide, the exposed sandy beach face during neap tide is about 30 m from the high water  
351 mark. In the following calculation, it is assumed that the width of the seepage face is 30 m.  
352 With the length of the shoreline approximately about 3.5 km, the amount of SGD should  
353 be around 8,000 m<sup>3</sup>/day for neap tide and 17,000 m<sup>3</sup>/day for spring tide. Result in nutrient  
354 analysis and nutrient loading to Plover Cove through SGD are given in Table 3.

## 355 **Conclusion**

356 Within Tolo Harbour, Plover Cove has been selected for SGD study. SGD flux has  
357 been estimated via continuous <sup>222</sup>Rn measurements and seepage meter. <sup>222</sup>Rn flux  
358 attributed to SGD has been obtained after correcting for tidal effect, atmospheric loss,  
359 sediment diffusion and mixing loss to the open sea. With terrestrial groundwater being  
360 selected, the amount of SGD is 8,000 m<sup>3</sup>/day during neap tide and 17,000 m<sup>3</sup>/day during  
361 spring tide. It has to point out that the estimated SGD include both components of  
362 terrestrial groundwater discharge as well as recirculated seawater.

363 Management of algal blooms has emphasized on external nutrient loading from rivers.  
364 Even most of the nutrient loading from rivers has been removed through the Tolo  
365 Harbour Action Plan, the total phytoplankton densities are still the highest among Hong  
366 Kong waters. In this study, nutrients discharged with SGD are conceived to be much  
367 more significant than all the other pathways in Plover Cove. Taking the width of the  
368 seepage area to be 30 m, nutrient loading on Plover Cove through SGD during neap tide  
369 and spring tide are: Total inorganic nitrogen 1,241 and 2,599 mol/day; Orthophosphate  
370 phosphorus 27.8 and 58.2 mol/day; Silica 185.9 and 388.5 mol/day. In terms of nutrient  
371 loadings per unit area, the amount of nitrate-nitrite nitrogen loading through SGD is about  
372 twice of that released from sediment diffusion obtained by Hu et al. (2001).  
373 Transformation along the groundwater flow path in the sediments may attenuate nutrient

374 composition in the SGD fluid but still, based on the result from this study, the current  
375 practice for the management of algal blooms in Tolo Harbour has to be reviewed and the  
376 control measures of groundwater contamination are obviously required.

377

## 378 **Acknowledgments**

379 This study was partially supported by a grant from the Research Grants Council of  
380 Hong Kong (HKU 7028/06P) and the Seed Funding within the Faculty of Science in The  
381 University of Hong Kong. The authors wish to thank staff from Department of Physics,  
382 HKU who helped in  $^{226}\text{Ra}$  measurement, staff from Department of Civil Engineering,  
383 HKU who helped in the nutrients analysis. The authors also appreciate students who  
384 assisted in the boat trips in the Tolo Harbour.

## References

- Addison, R. (1986), *Geology of Sha Tin: 1:20000 sheet 7*, Geotechnical Control Office, Civil Engineering Services Department, Hong Kong.
- Braja, M. D. (1999), *Principles of foundation engineering*, PWS Pub, Pacific Grove.
- Burnett, W. C., and H. Dulaiova (2003), Estimating the dynamics of groundwater input into the coastal zone via continuous radon-222 measurements, *Journal of Environmental Radioactivity*, 69, 21-35.
- Church, T. M. (1996), An underground route for the water cycle, *Nature*, 380, 579-580.
- Corbett, D. R., W. C. Burnett, P. H. Cable, and S. B. Clark (1998), A multiple approach to the determination of radon fluxes from sediments, *Journal of Radioanalytical and Nuclear Chemistry*, 236(1-2), 247-252.
- Durrige Co., Inc. (2001), *Manual for RAD AQUA*, Durrige Company.
- Dzhamalov, R. G. (1996), A conceptual model of subsurface water exchange between the continent and the sea, *Water Resources*, 23(2), 124-128.
- Environmental Protection Department (1994), *Marine Water Quality in Hong Kong in 1994*, Environmental Protection Department, Hong Kong.
- Environmental Protection Department (2004), *Marine Water Quality in Hong Kong in 2004*, Environmental Protection Department, Hong Kong
- Gallardo, A., and A. Marui (2006), Submarine groundwater discharge: an outlook of recent advances and current knowledge, *Geo-marine letters*, 26, 102-113.
- Geotechnical Control Office, Civil Engineering Services Department (1987), *Central New Territories*, Government Printer, Hong Kong.
- Geotechnical Control Office, Civil Engineering Services Department (1988), *North New Territories*, Government Printer, Hong Kong.

- Grant, C. J. (1989), *Permeability study – Lam Tsuen and Tolo Harbour Areas*, Environmental Protection Department, Hong Kong Government.
- Griggs, E. M., L. R. Kump, and J. K. Bohlke (2003), The fate of wastewater-derived nitrate in the subsurface of the Florida Keys: Key Colony Beach, Florida, *Estuarine, Coastal & Shelf Science*, 58, 517-539.
- Happell, J. D., J. P. Chanton, and W. J. Showers (1995), Methane transfer across the air-water interface in stagnant wooded swamps of Florida: Evaluation of mass-transfer coefficients and isotopic fractionation, *Limnology and Oceanography*, 40(2), 290-298.
- Hodgkiss, I. J., and B. S. S. Chan (1986), Studies on four streams entering Tolo Harbour, Hong Kong in relation to their impact on marine water quality, *Archiv für Hydrobiologie*, 108(2), 185-212.
- Hodgkiss, I. J., and K. C. Ho (1997), Are changes in N:P ratios in coastal waters the key to increased red tide blooms?, in *Asia-Pacific Conference on Science and Management of Coastal Environment*, edited by Y. S. Wong and Y. T. Fung, pp. 141-147, Kluwer Academic Publishers, Belgium.
- Hodgkiss, I. J., and W. W. S. Yim (1995), A case study of Tolo Harbour, Hong Kong, in *Eutrophic shallow estuaries and lagoons*, edited by A. J. McComb, pp. 41-57, CRC Press, Inc.
- Holmes, P. R. (1988), Tolo Harbour – the case for integrated water quality management in a coastal environment, *Journal of Institution of Water and Environmental Management*, 2, 171-179.
- Hu, W. F., W. Lo, H. Chua, S. N. Sin, and P. H. F. Yu (2001), Nutrient release and sediment oxygen demand in a eutrophic land-locked embayment in Hong Kong, *Environmental International*, 26, 369-375.

- Jiao, J. J., X. S. Wang, and S. Nandy (2005), Confined groundwater zone and slope instability in weathered igneous rocks in Hong Kong, *Engineering Geology*, 80, 71-92.
- Jiao, J. J., X. S. Wang, and S. Nandy (2006), Preliminary assessment of the impacts of deep foundations and land reclamation on groundwater flow in a coastal area in Hong Kong, China, *Hydrogeology Journal*, 14, 100-114.
- Johannes, R. E. (1980), The ecological significance of the submarine discharge of groundwater, *Marine Ecology Progress Series*, 3, 365-373.
- Kohout, F. A. (1966), Submarine springs: a neglected phenomenon of coastal hydrology, *Hydrology*, 26, 391-413.
- Lai, K. W., S. D. G. Campbell, and R. Shaw (1996), *Geology of the Northeastern New Territories: 1:20000 sheets 3 & 4*, Geotechnical Engineering Office, Civil Engineering Department, Hong Kong.
- Lambert, M. J., and W. C. Burnett (2003), Submarine groundwater discharge estimates at a Florida coastal site based on continuous radon measurements, *Biogeochemistry*, 66, 55-73.
- LaRoche, J., R. Nuzzi, R. Waters, K. Wyman, P. G. Falkowski, and D. W. R. Wallace (1997), Brown tide blooms in Long Island's coastal waters linked to international variability in groundwater flow, *Global Change Biology*, 3, 397-410.
- Lee, J. H. W., and F. Arega (1999), Eutrophication dynamics of Tolo Harbour, Hong Kong, *Marine Pollution Bulletin*, 39(1-12), 187-192.
- Lee, K. M., and P. C. C. Ng (1999), A geotechnical investigation of marine deposits in a nearshore seabed for land reclamation, *Canadian Geotechnical Journal*, 36(6), 981-1000.
- Li, H., and J. J. Jiao (2003), Tide-induced seawater-groundwater circulation in a multi-layered coastal leaky aquifer system, *Journal of Hydrology*, 274, 211-224.

- MacIntyre, S., R. Wanninkhof, and J. P. Chanton (1995), Trace gas exchange across the air-water interface in freshwater and coastal marine environments, in *Biogenic trace gases: Measuring emission from soil and water*, edited by P. A. Matson and R. C. Harriss, pp. 52-97, Blackwell Science, USA.
- Martens, C. S., G. W. Kipphut, and J. V. Klump (1980), Sediment-water chemical exchange in the coastal zone traced by in situ radon-222 flux measurements, *Science*, 208(4441), 285-288.
- Miller, D. C., and W. J. Ullman (2004), Ecological consequences of ground water discharge to Delaware Bay, United States, *Ground Water*, 42(7): 959-970.
- Moore, W. S. (1976), Sampling radium-228 in the deep ocean, *Deep-Sea Res.*, 23, 647-651.
- Moore, W. S. (1996), Large groundwater inputs to coastal waters revealed by  $^{226}\text{Ra}$  enrichments, *Nature*, 380, 612-614.
- Moore, W. S. (1999), The subterranean estuary: a reaction zone of ground water and sea water, *Marine Chemistry*, 65, 111-125.
- Peng, T. H., T. Takahashi, and W. S. Broecker (1974), Surface radon measurements in the North Pacific station Papa, *Journal of Geophysical Research*, 79, 1772-1780.
- Pilson, M. E. Q. (1998), *An introduction to the chemistry of the sea*, Prentice Hall, Upper Saddle River, New Jersey.
- Rutgers van der Loeff, M. M., and W. S. Moore (1999), Determination of natural radioactive tracers, in *Methods of seawater analysis*, edited by K. Grasshoff et al., pp. 365-398. Wiley-VCH, Weinheim, Germany.
- Ruxton, B. P., and L. Berry (1957), *Weathering of granite and associated erosional features in Hong Kong*, Geological Society of America, New York.

- Shum, K. T., and B. Sundby (1996), Organic matter processing in continental shelf sediments – the subtidal pump revisited, *Marine Chemistry*, 53, 81-87.
- Tam, S. W. (1980), *Environmental geological mapping of the Shatin Valley*, Department of Geography, Chinese University of Hong Kong, Hong Kong.
- Taniguchi, M., and H. Iwakawa (2001), Measurements of submarine groundwater discharge rates by a continuous heat-type automated seepage meter in Osaka Bay, Japan, *Journal of Groundwater Hydrology*, 43(4), 271-277.
- Taniguchi, M., W. C. Burnett, J. Christoff, C. F. Smith, R. J. Paulsen, D. O'Rourke, and S. Krupa (2003), Spatial and temporal distributions of submarine groundwater discharge rates obtained from various types of seepage meters at a site in northeastern Gulf of Mexico, *Biogeochemistry*, 66, 35-53.
- Tse, K. C. (2006), Estimation of submarine groundwater discharge into Tolo Harbour, M.Phil. Thesis, 106 pp., The University of Hong Kong, Hong Kong, 31 August.
- Ullman, W., and R. Aller (1981), Diffusion coefficients in nearshore marine sediments, *Limnology and Oceanography*, 27, 552-556.
- Webster, I. T., S. J. Norquay, F. C. Ross, and R. A. Wooding (1996), Solute exchange by convection within estuarine sediments, *Estuarine, Coastal and Shelf Science*, 42, 171-183.
- Whiteside, P. G. D (1984), Pattern of Quaternary sediments revealed during piling works at Sha Tin, Hong Kong, in *Geology of surficial deposits in Hong Kong*, edited by W. W. S. Yim, pp. 153-159, Geological Society of Hong Kong, Hong Kong.
- Xu, F. L., K. C. Lam, R. W. Dawson, S. Tao, and Y. D. Chen (2004), Long-term temporal-spatial dynamics of marine coastal water quality in the Tolo Harbor, Hong Kong, China, *Journal of Environmental Sciences*, 16(1), 161-166.

- Yim, W. W. S., and Q. Y. Li (1983), Sea-level changes and sea-floor surficial deposits off Chek Lap Kok, in *Geology of Surficial Deposits in Hong Kong: residual soil, colluvium, alluvium and marine deposits: programme, abstracts and excursion guide*, edited by W. W. S. Yim and A. D. Burnett, pp. 48-59, Geological Society of Hong Kong, Hong Kong.
- Yin, K. (2003), Influence of monsoons and oceanographic processes on red tides in Hong Kong waters, *Marine Ecology Progress Series*, 262, 27-41.
- Yung, Y. K., C. K. Wong, M. J. Broom, J. A. Ogden, S. C. M. Chan, and Y. Leung (1997), Long-term changes in hydrography, nutrients and phytoplankton in Tolo Harbour, Hong Kong, in *Asia-Pacific Conference on Science and Management of Coastal Environment*, edited by Y. S. Wong and Y. T. Fung, pp. 107-115, Kluwer Academic Publishers, Belgium.

## List of Tables

Table 1 Measurements of  $^{222}\text{Rn}$  in ambient air on 16th July 2005

Table 2 Estimated SGD fluxes

Table 3 Nutrients in porewater and nutrient loading to Plover Cove through SGD

## List of Figures

Figure 1 Map of Tolo Harbour

Figure 2 Sources and sinks of  $^{222}\text{Rn}$  in coastal waters (modified from Lambert and Burnett, 2003)

Figure 3 Temporal variation of  $^{222}\text{Rn}$  during neap tide

Figure 4 Temporal variation of  $^{222}\text{Rn}$  during spring tide

Figure 5 Wind speeds and atmospheric losses of  $^{222}\text{Rn}$  during neap tide

Figure 6 Wind speeds and atmospheric losses of  $^{222}\text{Rn}$  during spring tide

Figure 7 Net  $^{222}\text{Rn}$  flux during neap tide (The dashed line represents the mixing loss)

Figure 8 Net  $^{222}\text{Rn}$  flux during spring tide (The dashed line represents the mixing loss)

Figure 9 SGD fluxes during neap tide

Figure 10 SGD fluxes during spring tide

## Tables

**Table 1** Measurements of  $^{222}\text{Rn}$  in ambient air on 16th July 2005

Time	Conc. of $^{222}\text{Rn}$ (Bq/m <sup>3</sup> )
01:23	47.73
02:23	14.80
03:23	29.23
04:23	18.50
05:23	37.37
<b>Average</b>	<b>29.53</b>

**Table 2** Estimated SGD fluxes

### **During neap tide period**

Approach	SGD fluxes	Mean (cm/day)
<i><math>^{222}\text{Rn}</math> (SGD fluid represented by)</i>		
• Porewater	0-67.5	30.3
• Groundwater from nearshore wells	0-17.4	7.8
<i>Seepage meter</i>	0.9-40.1	8.0

### **During spring tide period**

Approach	SGD fluxes	Mean (cm/day)
<i><math>^{222}\text{Rn}</math> (SGD fluid represented by)</i>		
• Porewater	0-236	63.0
• Groundwater from nearshore wells	0-60.8	16.3
<i>Seepage meter</i>	1.0-144	9.3

**Table 3** Nutrients in porewater and nutrient loading to Plover Cove through SGD

Nutrients	Concentration ( $\mu\text{mol/L}$ )	Nutrient Loading to Plover Cove through SGD (mol/day)	
		Neap Tide	Spring Tide
Nitrite Nitrogen	0.8	6.6	13.7
Nitrate Nitrogen	78.6	643.7	1345.2
Ammonia Nitrogen	72.1	590.5	1234.0
Orthophosphate Phosphorus	3.4	27.8	58.2
Silica	22.7	185.9	388.5

Figures

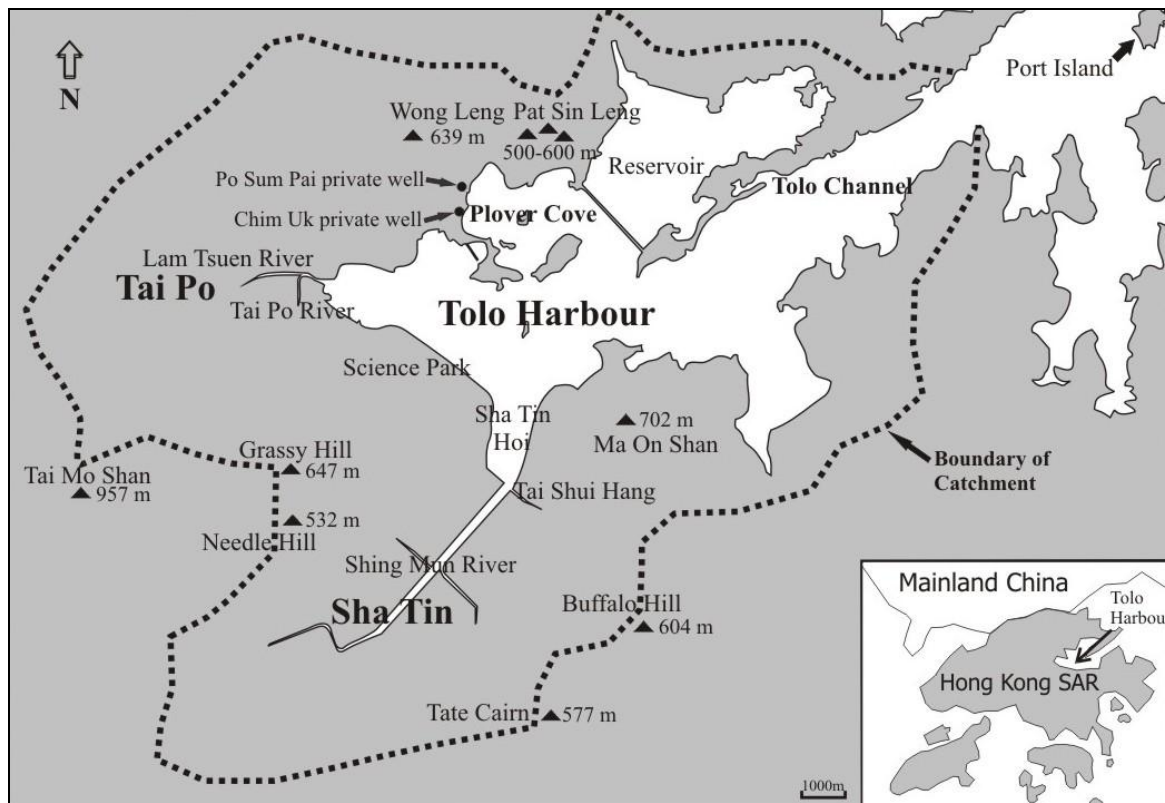


Figure 1 Map of Tolo Harbour

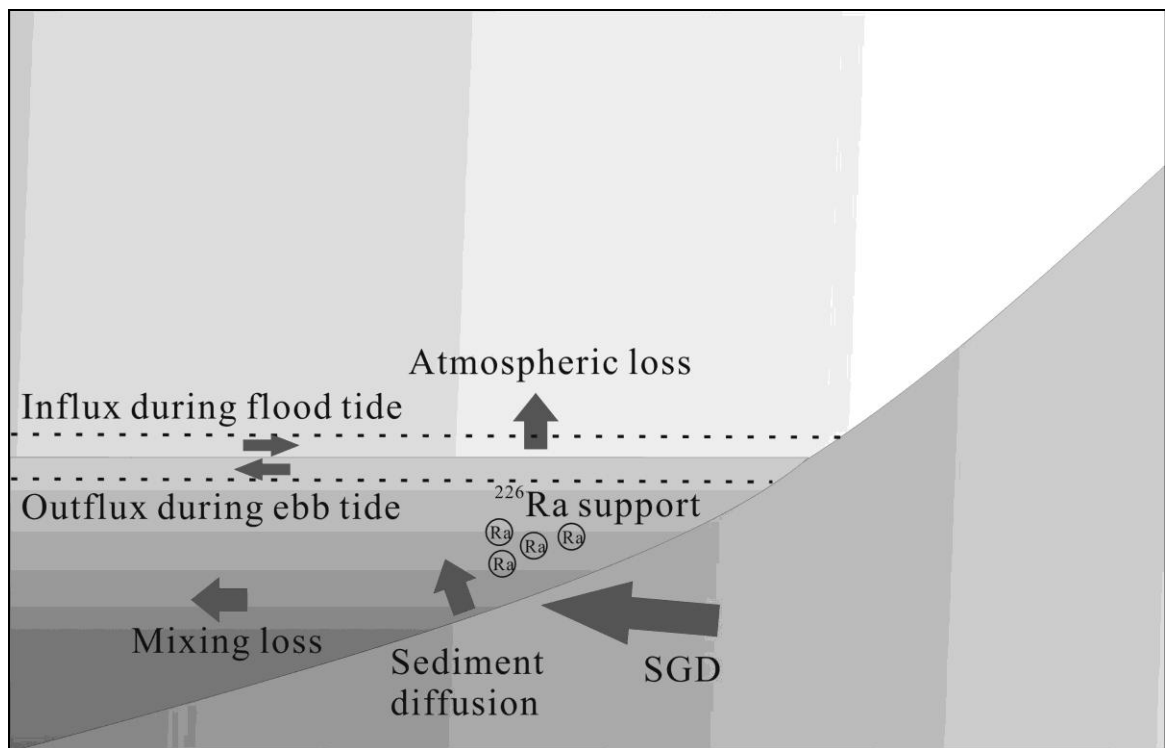


Figure 2 Sources and sinks of  $^{222}\text{Rn}$  in coastal waters (modified from Lambert and Burnett 2003)

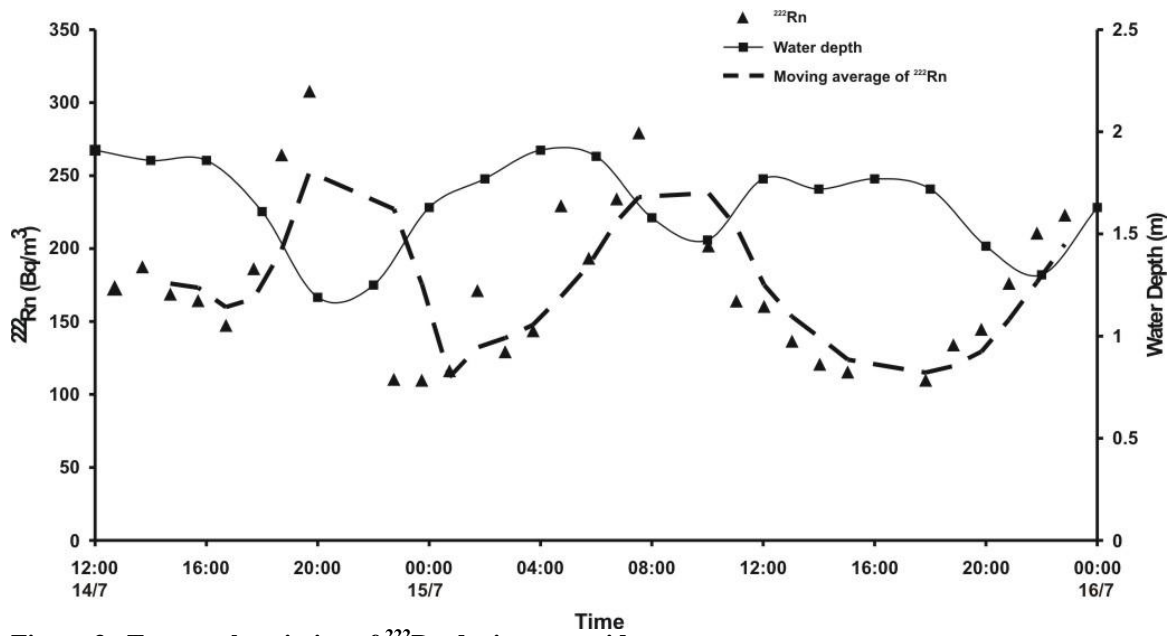


Figure 3 Temporal variation of  $^{222}\text{Rn}$  during neap tide

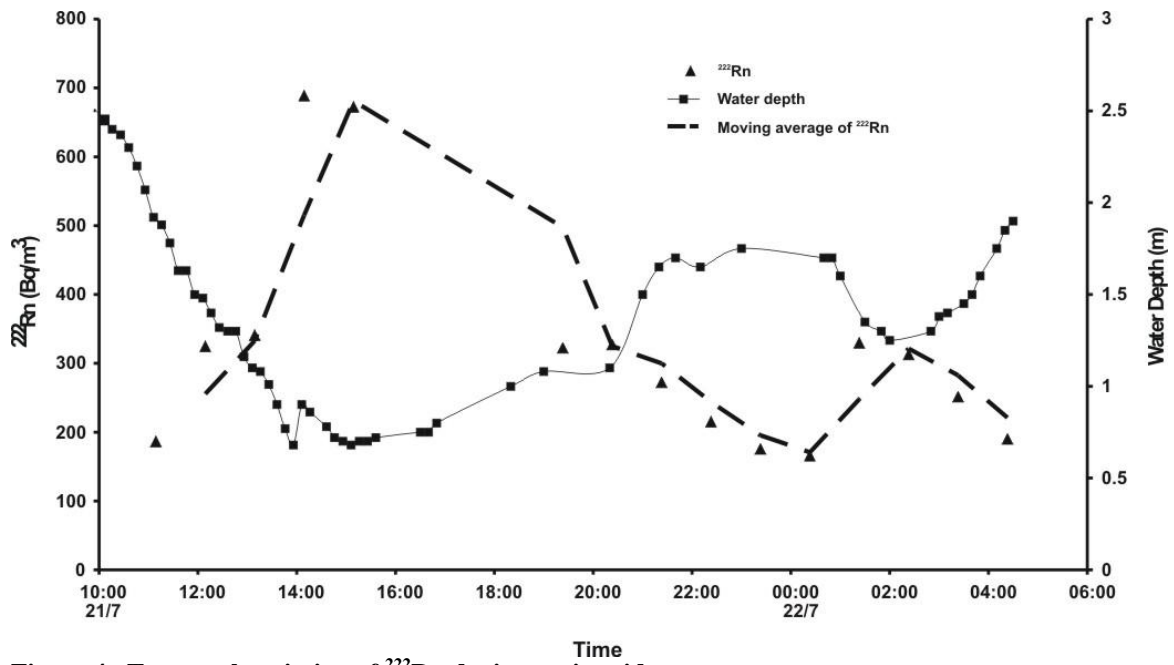


Figure 4 Temporal variation of  $^{222}\text{Rn}$  during spring tide

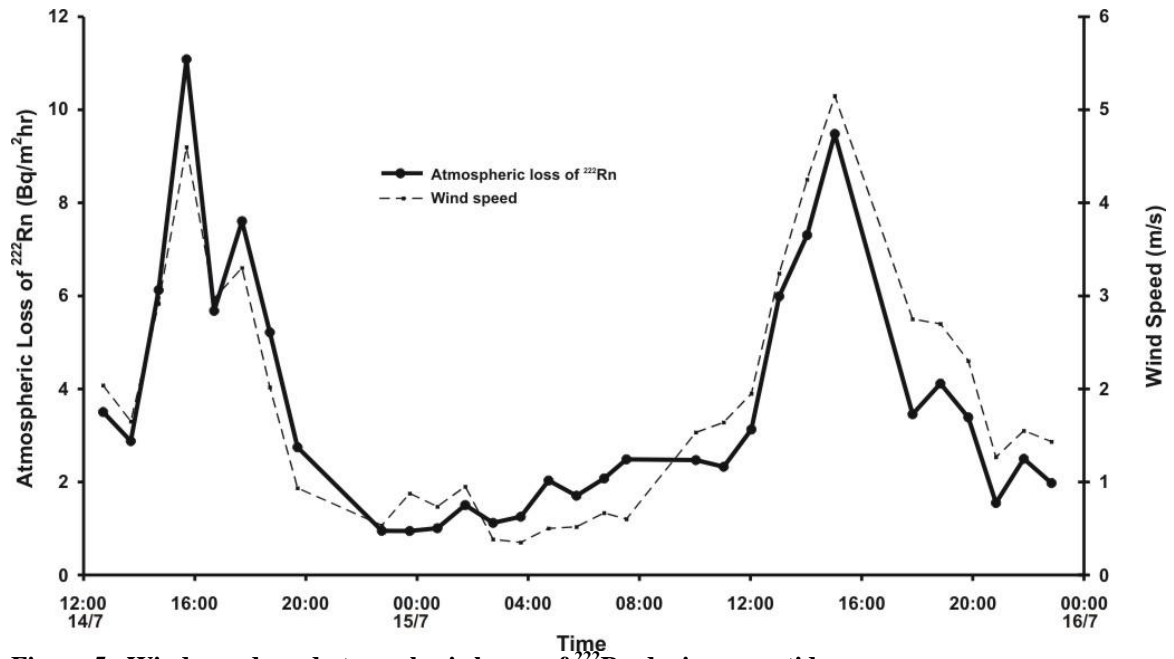


Figure 5 Wind speeds and atmospheric losses of  $^{222}\text{Rn}$  during neap tide

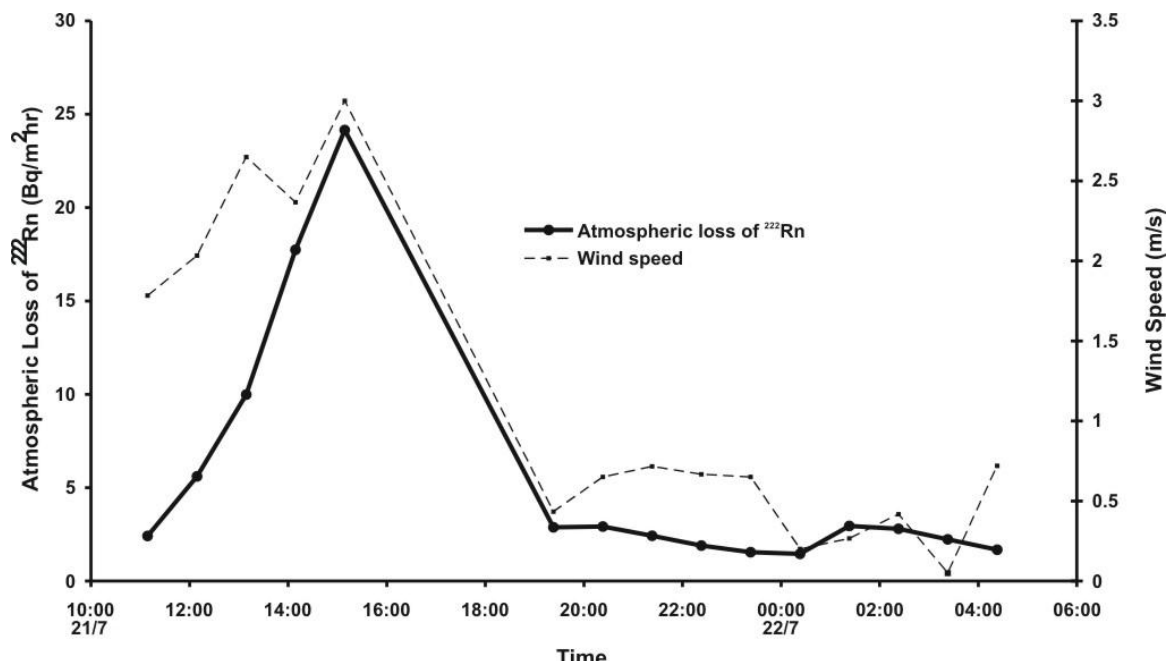


Figure 6 Wind speeds and atmospheric losses of  $^{222}\text{Rn}$  during spring tide

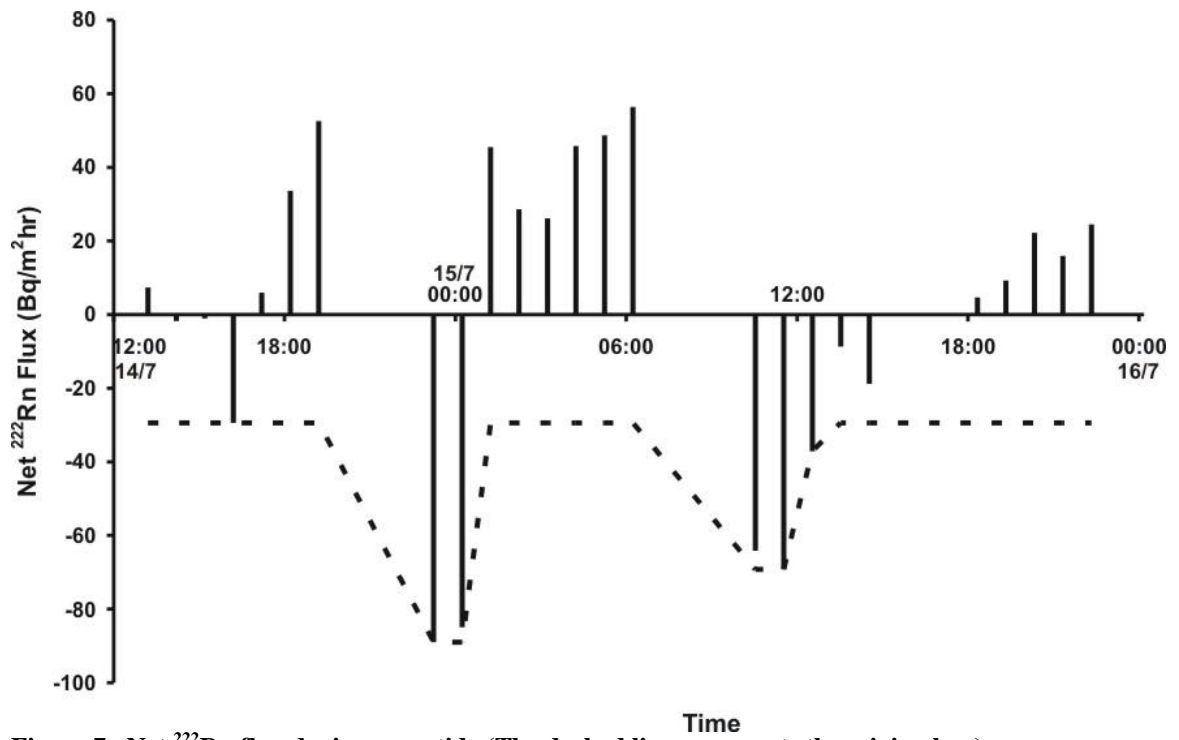


Figure 7 Net  $^{222}\text{Rn}$  flux during neap tide (The dashed line represents the mixing loss)

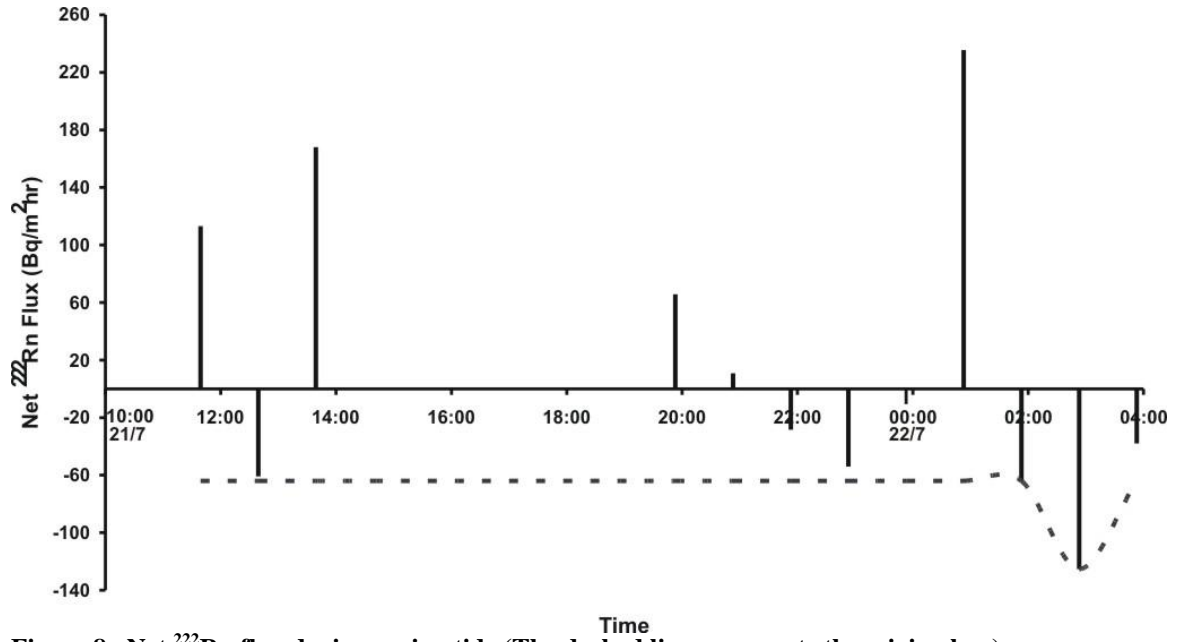


Figure 8 Net  $^{222}\text{Rn}$  flux during spring tide (The dashed line represents the mixing loss)

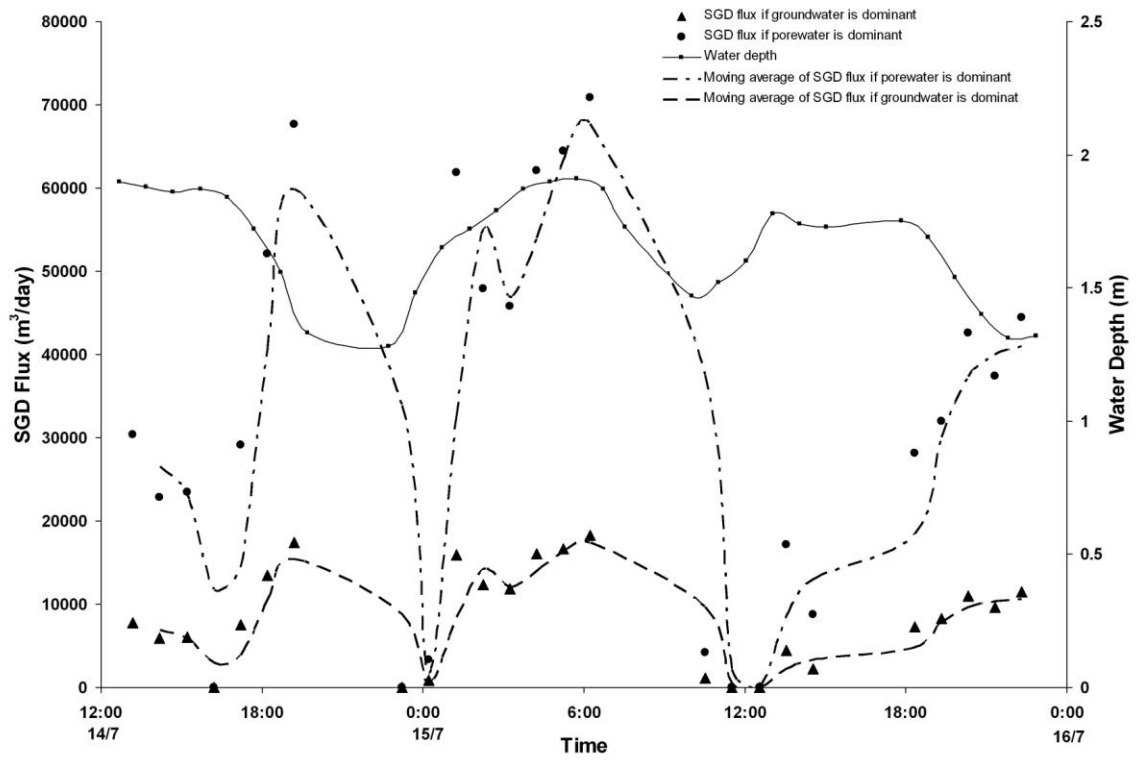


Figure 9 SGD fluxes during neap tide

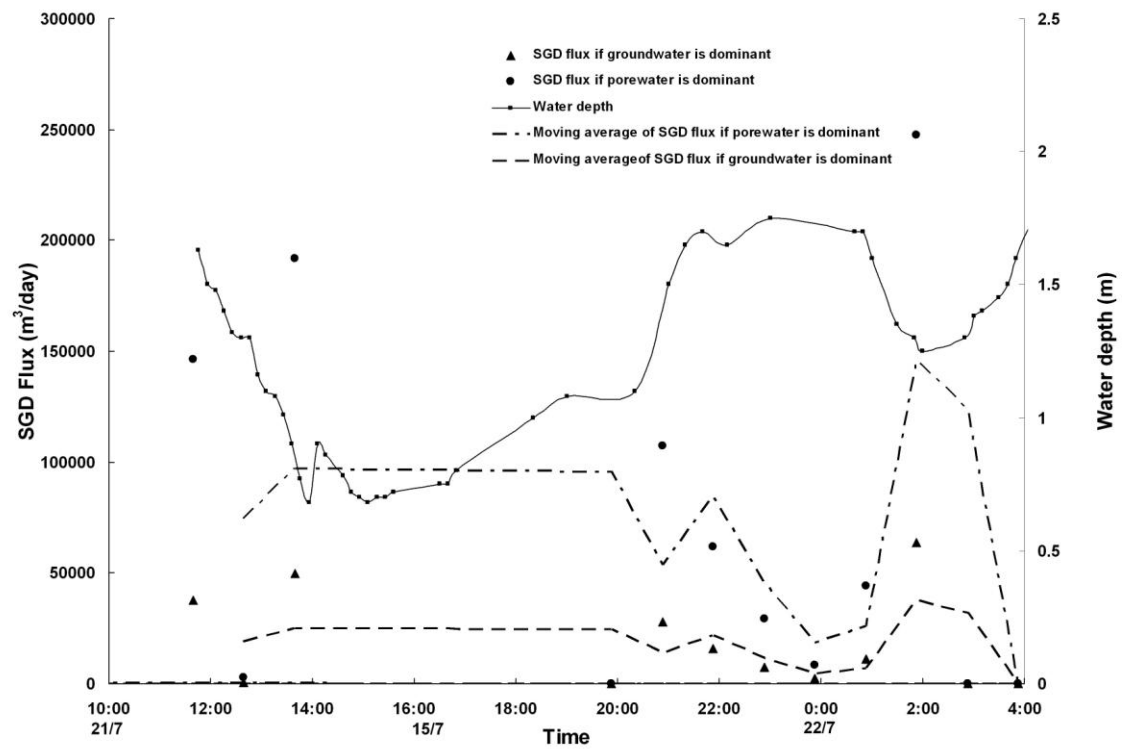


Figure 10 SGD fluxes during spring tide